Oncogene (2017) **36**, 5620–5630

www.nature.com/onc

OPEN

ORIGINAL ARTICLE

Targeting EphA2 impairs cell cycle progression and growth of basal-like/triple-negative breast cancers

W Song[1], Y Hwang[1], VM Youngblood[2], RS Cook[2,3], JM Balko[2,3], J Chen[1,2,3,4,5] and DM Brantley-Sieders[1,3]

Basal-like/triple-negative breast cancers (TNBCs) are among the most aggressive forms of breast cancer, and disproportionally affects young premenopausal women and women of African descent. Patients with TNBC suffer a poor prognosis due in part to a lack of molecularly targeted therapies, which represents a critical barrier for effective treatment. Here, we identify EphA2 receptor tyrosine kinase as a clinically relevant target for TNBC. EphA2 expression is enriched in the basal-like molecular subtype in human breast cancers. Loss of EphA2 function in both human and genetically engineered mouse models of TNBC reduced tumor growth in culture and *in vivo*. Mechanistically, targeting EphA2 impaired cell cycle progression through S-phase via downregulation of c-Myc and stabilization of the cyclin-dependent kinase inhibitor p27/KIP1. A small molecule kinase inhibitor of EphA2 effectively suppressed tumor cell growth *in vivo*, including TNBC patient-derived xenografts. Thus, our data identify EphA2 as a novel molecular target for TNBC.

Oncogene (2017) **36,** 5620–5630; doi:10.1038/onc.2017.170; published online 5 June 2017

INTRODUCTION

Triple-negative breast cancers (TNBCs) are characterized by lack of estrogen and progesterone nuclear hormone receptor (ER/PR) expression, as well as lack of the human epidermal growth factor receptor-2, (HER2).[1] TNBCs often, though not always, overlap with the basal-like intrinsic molecular subtype.[2] Though only ~15–20% of all breast cancers are diagnosed as basal-like/triple-negative (referred to herein for simplicity as TNBC), TNBC disproportionately affects young premenopausal women, as well as women of African descent, and is difficult to treat.[3,4] These tumors are also associated with a poor prognosis, high recurrence risk, and poor disease-free survival relative to other breast cancer subtypes. In fact, the median survival of patients with metastatic TNBC is just 13 months, and almost all patients with metastatic TNBC die in spite of treatment with systemic chemotherapy, the only treatment option currently available due to a lack of validated, actionable molecular targets for therapy.[3–5]

The Eph family of receptor tyrosine kinases (RTKs) are key regulators of development and disease, including cancer (reviewed in Kullander and Klein,[6] Pasquale[7,8]). These molecules can enhance or suppress tumorigenesis and progression depending upon their mode of activation. For example, ligand-dependent signaling induced by ephrin-A1 is suppressive. Ephrin-A1 ligand binding induces receptor clustering and initial activation followed by subsequent receptor internalization, downregulation, and inhibition of MAPK and Akt signaling pathways in breast and other tumor types.[9] In contrast to ligand-induced signaling, EphA2 can be activated by interaction with other cell-surface receptors, such as EGFR and HER2/ErbB2, in cancer cells, amplifying MAPK, Akt and Rho family GTPase activities.[10,11] Indeed, ratios of *ephA2/ephrin-A1* expression in human breast cancer support ligand-independent signaling.[12] While overexpression of EphA2 and other Eph receptors has been linked to poor overall and recurrence-free survival (RFS) in breast cancers across all subtypes,[12] these global profiling studies did not address the role of Eph family members within specific molecular subtypes.

Here, we report that EphA2 expression is enriched in the basal-like breast cancer molecular subtype and correlates with poor RFS in human TNBC. Loss of EphA2 function reduced proliferation at the level of S-phase cell cycle progression in both transgenic mouse and human cell line models of TNBC in culture and *in vivo*. Mechanistically, we link EphA2-mediated regulation of c-Myc and p27/KIP1 cyclin-dependent kinase (cdk) inhibitor to TNBC proliferation. Finally, we determined that an EphA2 small molecule inhibitor significantly reduced tumor growth in TNBC models, including patient-derived xenografts (PDXs). Thus, EphA2 represents a novel, clinically relevant molecular target in TNBC that could be developed to impair pro-proliferation pathways that drive malignancy in this aggressive breast cancer subtype.

RESULTS

EphA2 negatively correlates with overall and RFS and is enriched in the TNBC molecular subtype

Previous analyses of human breast tumor microarray data sets and tissue microarrays (TMAs) revealed that EphA2 is elevated in human breast cancer relative to normal/adjacent breast tissue controls, and that high expression levels correlate with poor patient survival across molecular subtypes.[12] When we interrogated The Cancer Genome Atlas breast cancer data sets stratified by PAM50 molecular subtype,[13] we found enrichment of high-level *EPHA2* expression in the basal-like molecular subtype coincident with lower level ephrin-A1 (*EFNA1*) ligand expression (Figure 1a). Moreover, analysis of patient data[14] selected for ER^-/PR^-

[1]Department of Medicine, Vanderbilt University School of Medicine, Nashville, TN, USA; [2]Department of Cancer Biology, Vanderbilt University School of Medicine, Nashville, TN, USA; [3]Vanderbilt-Ingram Cancer Center, Vanderbilt University School of Medicine, Nashville, TN, USA; [4]Department of Cellular and Developmental Biology, Vanderbilt University School of Medicine, Nashville, TN, USA and [5]Veterans Affairs Medical Center, Tennessee Valley Healthcare System, Nashville, TN, USA. Correspondence: Dr DM Brantley-Sieders, Department of Medicine, Vanderbilt University School of Medicine, T-3107A MCN, 1161 21st Avenue South, Nashville, TN 37232-2681, USA or Dr J Chen, Vanderbilt University School of Medicine, T-3207E MCN, 1161 21st Avenue South, Nashville, TN 37232-2681, USA.
E-mail: dana.brantley@vanderbilt.edu or jin.chen@vanderbilt.edu
Received 10 November 2016; revised 27 April 2017; accepted 1 May 2017; published online 5 June 2017

basal-like cancers revealed a significant correlation between high *ephA2* expression and reduced RFS probability (Figure 1b). We also observed high-level expression of EphA2 protein in 65% of cases from a human TNBC TMA relative to 20% of control (normal/hyperplastic and benign fibroadenoma) samples from previously analyzed human breast cancer TMA (Figure 1c).[12] Consistent with these data, EphA2 expression was elevated in several human TNBC cell lines relative to normal human mammary epithelial cells (Supplementary Figure S1a). Together, these data support clinical relevance of EphA2 in TNBC and clinical outcome.

EphA2 is required for proliferation in human TNBC lines

To determine the role of EphA2 in TNBC, we generated stable short hairpin RNA (shRNA) knockdown sublines in six independent human TNBC lines (Figures 2a and b). Knockdown was >90% in shEphA2 lines, as determined by immunoblot analysis (Figure 2b; Supplementary Figure S1b). We assessed proliferation and survival in three cell lines that displayed significantly decreased growth in MTT assays upon loss of EphA2 (Figure 2a) relative to vector control. Loss of EphA2 expression significantly reduced proliferation, as measured by BrdU incorporation, in MDA-MB-231, HCC1395 and BT549 TNBC cell lines *in vitro* (Figures 2c and d). Apoptosis, as assessed by terminal deoxynucleotidyl transferase (TdT) dUTP nick-end labeling (TUNEL) analysis, was unaffected by loss of EphA2 (Figure 2e). We validated the effects of EphA2 knockdown on TNBC cell growth by two individual shRNAs versus shRNA targeting GFP control to confirm specificity of EphA2 targeting (Supplementary Figures S1b and c).

Consistent with proliferation data *in vitro*, tumor growth was significantly decreased in EphA2 knockdown MDA-MB-231 and BT549 xenografts *in vivo*. For these experiments, EphA2 knockdown cells were injected orthotopically into left inguinal mammary fat pads of nude female mice, and growth was compared to vector control cells injected into the right contralateral inguinal mammary fat pads. We observed a significant reduction in tumor volume between 1 and 2 weeks post injection for EphA2 knockdown tumors relative to controls (Figure 3a). Tumors were collected after 2 weeks, processed for histology, and sections stained for Ki67 to score proliferation (Figures 3b and c), cleaved caspase 3 (Cl-Casp3) to score apoptosis (Supplementary Figure S2a), and CD31 to score microvascular density (Supplementary Figure S2b). While proliferation was significantly reduced in EphA2 knockdown xenografts (Figures 3b and c), apoptosis levels were unaltered (Supplementary Figure S2a), consistent with growth of TNBC lines *in vitro*. Loss of EphA2 in xenografts did not significantly alter microvascular density *in vivo* (Supplementary Figure S2b).

EphA2 is required for proliferation in a mouse model of basal-like breast cancer

To validate our findings in human TNBC cell line models, we tested the impact of EphA2 loss in the C3(1)-TAg mouse model of basal-like breast cancer. In this model, SV40 virus large T-antigen is driven by the 5′ flanking region of the C3 (1) component of the rat prostate steroid-binding protein, which produces basal-like mammary adenocarcinomas with 100% penetrance in female mice.[15,16] Hyperplastic tissue and tumors from these animals express EphA2 at higher levels than normal mammary epithelial tissue (Supplementary Figures S3a and b), suggesting that EphA2 might play a role in malignant progression in this model. To test this hypothesis, we crossed C3-TAg transgenic mice with EphA2-

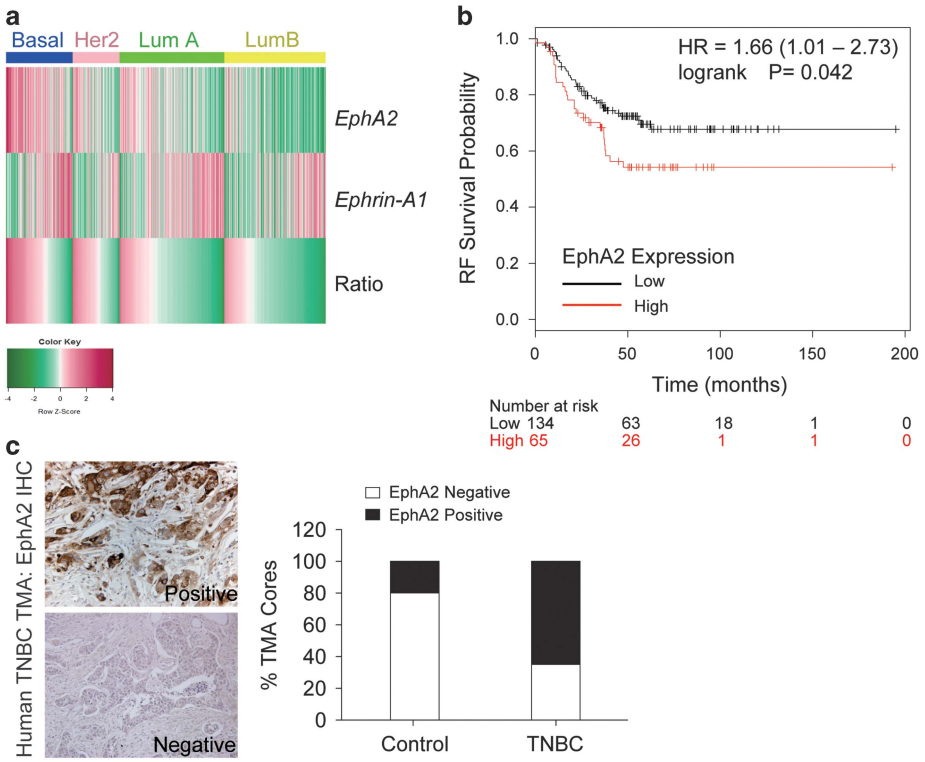

Figure 1. Clinical relevance of EphA2 in basal-like/triple-negative breast cancer. (**a**) Heat map analysis of *EPHA2* and *EFNA1* messenger RNA expression in breast cancer microarray data from The Cancer Genome Atlas (TCGA) stratified by PAM50 molecular subtype revealed *EPHA2* enrichment in the basal-like subtype concomitant with mutually exclusive *EFNA1* expression. (**b**) Kaplan–Meier analysis of data set with microarray profiles from 316 ER^{-}/PR^{-} human basal-like breast cancer samples (KMplot.com). Upper tertile expressing highest *EPHA2* levels (red line) significantly correlated with lower recurrence-free (RF) survival probability. (**c**) Analysis of human TNBC tissue microarray (TMA) revealed high-level EphA2 protein expression in 65% of samples (31 out of 48 positive/high) relative to 20% of control (normal/hyperplastic and benign fibroadenoma; 2 out of 10 positive/high) samples from previously analyzed human breast cancer TMA. HR, hazard ratio.

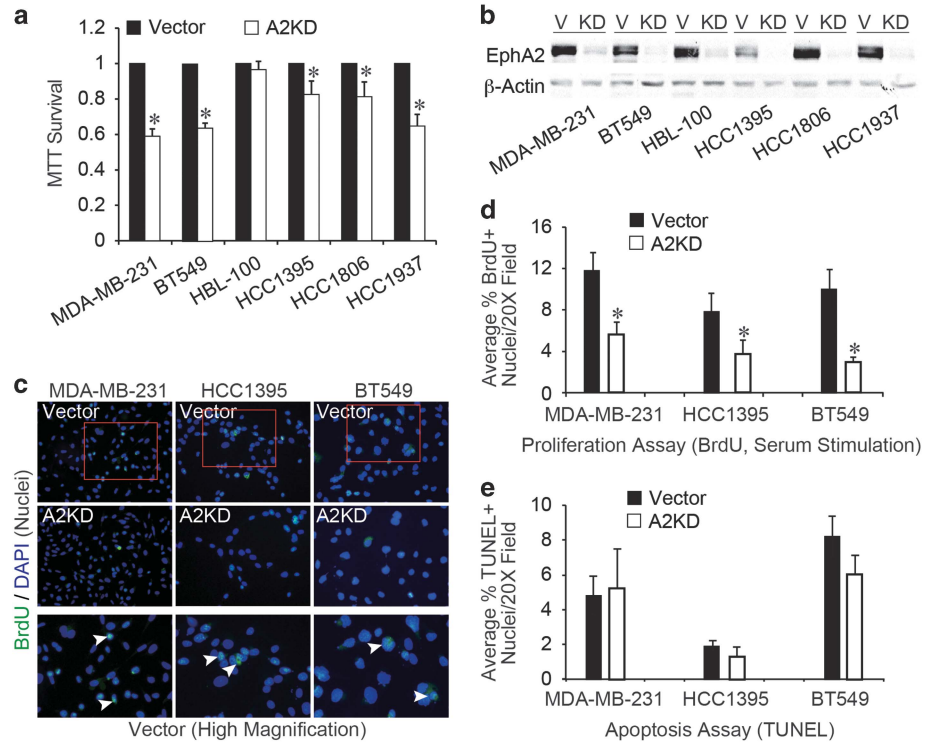

Figure 2. EphA2 knockdown impairs proliferation in human TNBC cell lines. (**a**) Growth of TNBC lines stably expressing lentiviral control vector or EphA2 shRNA (EphA2 KD) was assessed by MTT assay. Loss of EphA2 expression significantly impaired growth in MDA-MB-231, BT549, HCC1395, HCC1806 and HCC1937 lines (*$P < 0.05$, Student's *t*-test). (**b**) EphA2 knockdown was confirmed in human TNBC cell lines via immunoblot analysis. (**c**) MDA-MB-231, HCC1395 and BT549 lines were starved and then serum-stimulated in the presence of BrdU to mark proliferating cells. BrdU-positive nuclei were detected using a FITC-conjugated anti-BrdU antibody (green, arrowheads) and all nuclei were visualized using DAPI counterstain (blue). (**d**) Proliferation (% $BrdU^+$ nuclei/total nuclei) was significantly reduced in EphA2 KD lines relative to controls (*$P < 0.05$, Student's *t*-test). Boxed areas in upper vector control panels indicate areas of high magnification displayed in lower panels. (**e**) For apoptosis assays, cells were starved for 48 h and then subjected to TUNEL analysis. Apoptosis (% $TUNEL^+$ nuclei/total nuclei) was not affected by EphA2 knockdown (not significant, Student's *t*-test). $N = 3$ independent experiments with triplicate biological replicates for each line.

deficient mice[10] to generate cohorts of wild type, EphA2 heterozygous and EphA2 homozygous null C3-TAg female mice. Relative to wild-type control littermates, EphA2-deficient female mice developed significantly smaller tumors (Figures 4a and b) with reduced tumor epithelial density (Figure 4c). Moreover, tumor epithelium from EphA2-deficient animals displayed significantly fewer mitotic figures (Figure 4a, green arrowheads; Figure 4c). Consistent with data derived from human cell lines, deletion of one or both copies of EphA2 in C3-TAg tumors resulted in a significantly reduced tumor proliferation index relative to tumors produced by wild-type controls, as measured by nuclear Ki67 (Figure 4d). Interestingly, reduced proliferation only correlated with a significant decrease in tumor volume for EphA2-deficient animals (~15% reduction) and not for heterozygous littermates (~8% reduction), suggesting only that loss of both copies of EphA2 is sufficient to significantly impair tumor growth *in vivo*. Alternatively, a higher degree of variability in tumor volume for +/− samples (Figure 4b, error bars) perhaps masked potential differences between +/+ and +/− tumors. In addition, most +/− tumors appeared cystic in hemotoxylin and eosin-stained sections (~83%), which could have increased tumor volume measurements independently of tumor cell proliferation.

Consistent with cell line and xenograft data, we observed no significant differences in apoptosis levels between wild-type, heterozygous and EphA2-deficient tumors based on staining for cleaved caspase 3 (Supplementary Figure S4a). EphA2 has an established role in promoting tumor neovascularization in several cancer models, including breast,[10,17,18] which might also affect tumor growth in EphA2-deficient animals and prompted us to assess tumor microvascular density in the C3-TAg model. We did not observe any significant differences in microvascular density based on CD31 staining in tumor sections from wild-type versus EphA2-deficient littermate controls (Supplementary Figure S4b), suggesting that defective tumor cell proliferation most likely accounts for decreased tumor volume and growth.

We previously reported that loss of EphA2 transiently impairs branching morphogenesis in normal mammary epithelium during post-natal purbertal development,[19] a phenotype that persisted in some adult EphA2-deficient female mice co-expressing the MMTV-Neu transgene.[10] To determine if post-natal branching and outgrowth defects contribute to decreased tumorigenesis and growth, we quantified the frequency of branching defects in non-transgenic wild-type versus EphA2-deficient littermates and hyperplasia frequency in wild-type versus EphA2-deficient C3-TAg-positive female mice. We observed that 57% of 12-week-old non-transgenic EphA2-deficient littermate controls displayed mild to moderate branching defects relative to non-transgenic EphA2 wild-type littermates. However, rates of hyperplasia were comparable between 12-week-old wild-type and EphA2-deficient C3-TAg mice (Supplementary Figure S4c), and we observed no differences in tumor latency between genotypes (data not shown). These data suggest that developmental defects in epithelial branching do not directly impact malignant progression in this model.

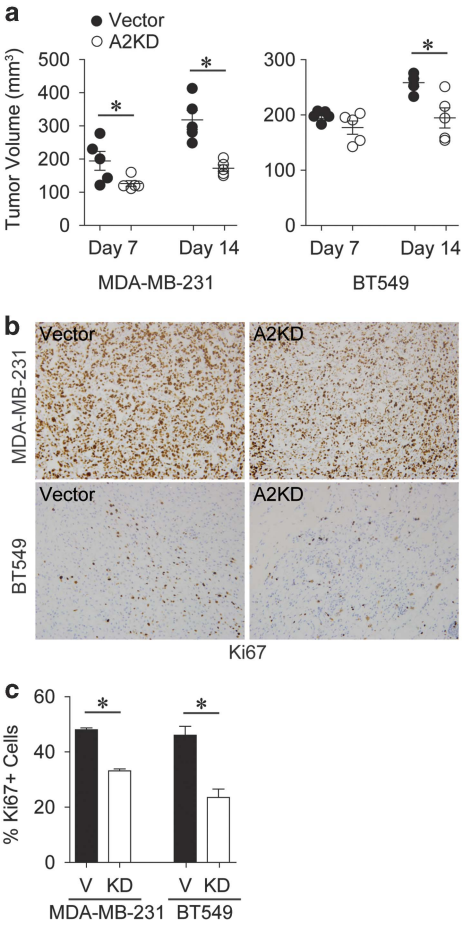

Figure 3. EphA2 knockdown impairs proliferation in human TNBC lines *in vivo*. (**a**) MDA-MB-231 and BT549 vector control and EphA2 knockdown (A2KD) lines were orthotopically injected into the mammary fat pads of nude female mice and tumor volume was measured over the course of 2 weeks. EphA2 knockdown tumors were significantly smaller than vector controls at 1 and/or 2 weeks post injection ($N = 5$ tumors/condition; $^*P < 0.05$, ANOVA). (**b**, **c**) Histologic analyses of tumor sections for Ki67, a marker of proliferation, revealed a significant decrease in proliferation index (%Ki67$^+$ nuclei/total nuclei; $^*P < 0.05$, Student's *t*-test) for EphA2$^{-/-}$ tumors relative to controls. ANOVA, analysis of variance.

To determine if defects produced by EphA2 loss were intrinsic to tumor epithelium, we isolated primary tumor cells from wild-type and EphA2-deficient C3-TAg mice, and assessed growth and colony morphology in three-dimensional Matrigel culture.[10,20] While wild-type C3-TAg cells formed large, irregular colonies, colonies formed by EphA2-deficient cells were significantly smaller and displayed a more uniform spheroid morphology (Figures 4e and f). Restoring EphA2 expression via adenoviral EphA2 delivery rescued the phenotype in EphA2-deficient C3-TAg colonies (Figures 4e–g). These data support the epithelial intrinsic, pro-proliferative function of EphA2 in basal-like/TNBC *in vivo*.

EphA2 promotes basal-like breast cancer cell growth through activation of c-Myc and downregulation of p27/KIP1

To further characterize the role of EphA2 in TNBC proliferation, we compared cell cycle progression in propidium iodide-stained control versus EphA2 knockdown cell lines via fluorescence activated cell sorting (FACS) analysis. Cells were starved and then stimulated with serum over a time course prior to labeling and FACS (Figure 5a). EphA2 knockdown MDA-MB-231 displayed a decrease in the percentage of cells in S-phase relative to vector controls after 15 h of serum stimulation. HCC1395 knockdown cells also showed a decrease in the percentage of cells in S-phase after 15 h of serum stimulation, as well as in unstimulated cells, relative to controls. While trends were variable in diploid BT549 cells, aneuploid knockdown cells displayed a decrease in the percentage of cells in S-phase after serum stimulation and in unstimulated cells. Thus, all three human EphA2 knockdown lines showed a general decrease in the percentage of cells in S-phase relative to vector controls (Figure 5a).

Consistent with these data, we observed altered expression and/or activity in key G_1/S cell cycle checkpoint regulators. Levels of positive regulators c-Myc and cyclin E2 were reduced upon EphA2 knockdown in human TNBC lines or knockout in C3-TAg tumor cells (Figures 5b and c). While we detected no change in expression or phosphorylation of cdk2 (Supplementary Figure S5), levels of p27/KIP1 cdk2/4 inhibitor were markedly elevated in two out of three EphA2 knockdown human TNBC lines (MDA-MB-231 and HCC1395) and in EphA2-deficient C3-TAg cells (Figures 5b and c). We confirmed these expression patterns in TNBC cells using individual EphA2 shRNA versus shRNA targeting GFP (Supplementary Figure S1b). We did not observe differences in expression of other cell cycle regulators/tumor suppressors (for example, cyclin B1, p53) in EphA2-deficient C3-TAg cells, though EphA2-deficient cells showed decreased levels of phosphorylated Erk and Akt growth regulators (Supplementary Figure S5), consistent with previous studies in breast cancer models.[10] Loss of EphA2 also appeared to reduce levels of phosphorylated retinoblastoma gene product (Rb; Figures 5b and c), another negative regulator of G_1/S progression that is inactivated by hyperphosphorylation.[21] Together, these data suggest that EphA2 regulates TNBC proliferation at the level of S-phase cell cycle progression through modulation of c-Myc, p27/KIP1 and cyclin E2 expression.

To validate the functional link between EphA2 and these cell cycle regulators, we overexpressed EphA2 in wild-type C3-TAg cell lines. EphA2 overexpression significantly increased colony size in three-dimensional spheroid culture (Figures 5d and e). Consistent with our loss-of-function studies, EphA2 overexpression elevated c-Myc levels in wild-type C3-TAg cells, as well as elevating levels of cyclin E2 and phosphorylated Rb (Figure 5f). We also over-expressed c-Myc (Figures 5d–f) by adenoviral transduction and knocked out p27/KIP1 (Figures 5g–i) by lentiviral CRISPR/Cas9 in EphA2-deficient C3-TAg lines. Restoring c-Myc expression or ablating p27/KIP1 rescued growth of EphA2-deficient cells in three-dimensional spheroid culture, increasing colony size to comparable levels observed in wild-type C3-TAg (Figures 5d–h). These data confirm a functional link between EphA2 and c-Myc/p27 stability in basal-like breast cancer growth. In addition, analysis of human TNBC TMAs (Supplementary Figures S6a and b) revealed (i) a significant correlation between EphA2 receptor expression and c-Myc expression; (ii) an inverse correlation between EphA2 and p27/KIP1 levels; (iii) and an inverse correlation between EphA2/c-Myc expression and p27/KIP1 expression. These data support the clinical relevance of EphA2-dependent regulation of S-phase cell cycle/growth signaling factors in basal-like/TNBC.

Targeting EphA2 impairs growth *in vitro* and in clinically relevant TNBC models *in vivo*

To determine the impact of targeting EphA2 on TNBC, we treated TNBC cells with a small molecule tyrosine kinase inhibitor of EphA2, ALW-II-41-27, which has been shown to effectively inhibit EphA2 function in lung cancer models.[22,23] Relative to analog control compound NG-25, ALW-II-41-27 significantly impaired growth of MDA-MB-231 cells in MTT assays in a dose-dependent

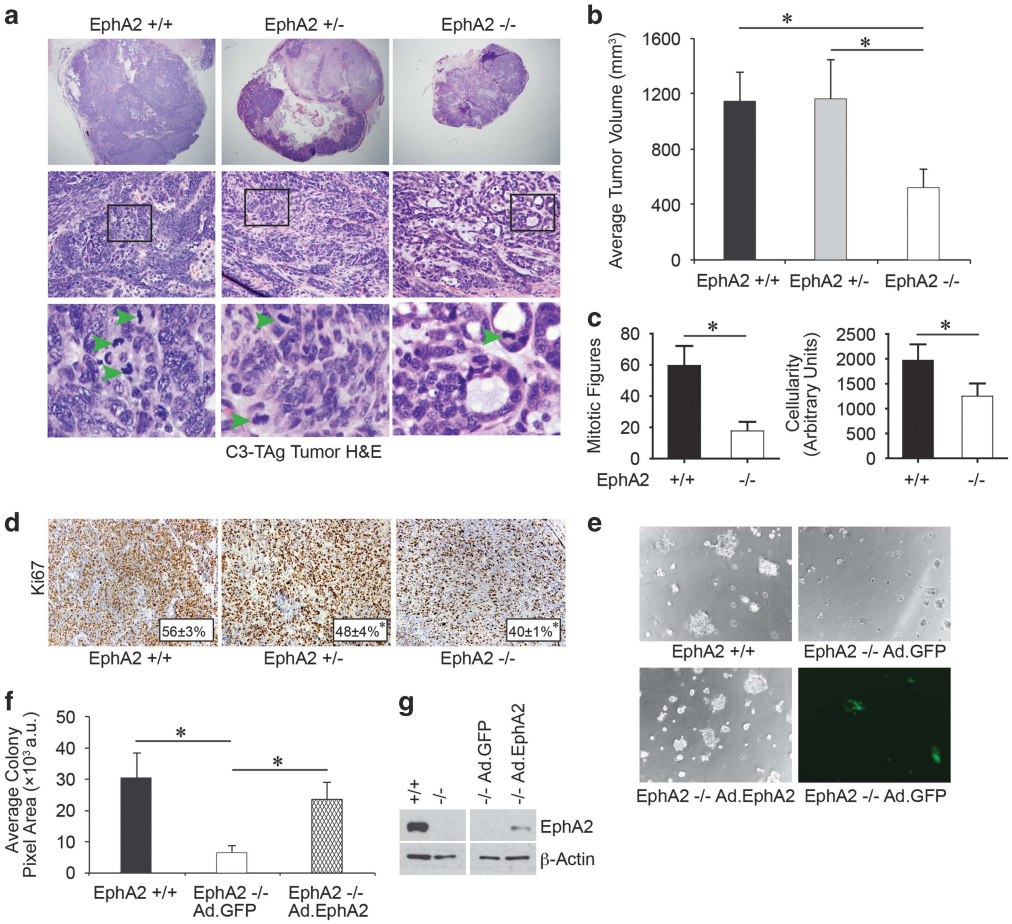

Figure 4. EphA2-deficiency impairs growth and progression in the C3-TAg transgenic model of basal-like breast cancer *in vivo*. We crossed C3-TAg mice with EphA2-deficient mice, generating a cohort of C3-TAg wild-type ($EphA2^{+/+}$), heterozygous ($EphA2^{+/-}$) and EphA2-deficient (EphA2-/-) mice. (**a**) EphA2-deficient mice formed significantly smaller tumors than wild-type or heterozygous littermates. (**b**) Tumor volume was significantly decreased in EphA2-deficient animals relative to littermate controls ($N = 9^{+/+}$, $11^{+/-}$ and $9^{-/-}$ animals; $^*P < 0.05$, one-way ANOVA). (**c**) Morphometric analysis of hematoxylin and eosin-stained tumor sections revealed a significant decrease in mitotic figures (green arrowheads, **a**) in $EphA2^{-/-}$ tumors relative to +/+ controls, as well as decreased cellularity ($n = 6$ independent tumors/genotype; $^*P < 0.05$ Student's *t*-test). (**d**) Histologic analyses of tumor sections for proliferation marker Ki67 revealed a significant decrease in proliferation index (% Ki67+ nuclei/total nuclei; $^*P < 0.05$, Student's *t*-test) for $EphA2^{-/-}$ tumors relative to controls. (**e**, **f**) Primary tumor cells from $EphA2^{+/+}$ and $EphA2^{-/-}$ C3-TAg tumors were isolated and grown in three-dimensional spheroid cultures on Matrigel for 10–12 days. $EphA2^{-/-}$ cells formed significantly smaller colonies than $EphA2^{+/+}$ cells (**e**, **f**; $^*P < 0.05$, Student's *t*-test). Expression of EphA2 in $EphA2^{-/-}$ cells via adenoviral transduction rescued colony size (**e**, **f**; $^*P < 0.05$, Student's *t*-test) relative to adenovirus GFP control (expression confirmed by fluorescence analysis, lower right panel, **e**), restoring growth to near wild-type C3-TAg levels. $N = 3$ independent experiments with triplicate biological replicates for each cell line. (**g**) EphA2-deficiency and overexpression of EphA2 following adenoviral transduction were confirmed by immunoblot analysis.

manner after 72 h in culture (Figure 6a). Consistent with EphA2 shRNA knockdown, ALW-II-41-27 treatment reduced levels of c-Myc and cyclin E2 while elevating p27/KIP1 in MDA-MB-231 relative to control (Figure 6b). Similar results were obtained in wild-type C3-TAg tumor cells (Figures 6c and d). To validate EphA2 targeting, we assessed EphA2 phosphorylation in MDA-MB-231 and C3-TAg cells treated with inhibitor or analog control. ALW-II-41-27 significantly reduced EphA2 phosphorylation at tyrosine 588 in the human TNBC line (Figure 6b). The EphA2 inhibitor also decreased tyrosine phosphorylation of EphA2 in C3-TAg cells stimulated with soluble ephrin-A1 ligand (Figure 6e).

To test for off-target effects, we treated wild-type and EphA2-deficient C3-TAg cells with control NG-25 or ALW-II-41-27 in three-dimensional spheroid culture and quantified colony size and morphology. Previous studies from Nathanael Gray's laboratory, in which ALW-II-41-27 was developed, tested ALW-II-41-27 for affinity and inhibition of EphA2 kinase activity relative to other Eph RTK family members and other kinases. ALW-II-41-27 exhibited marked specificity for EphA2 relative to other kinases.[24] Studies from our laboratory using cell line and mouse models of non-small cell lung cancer confirmed EphA2 targeting.[22,23] A more recent study, however, reported that ALW-II-41-27 inhibits RET tyrosine kinase activity and function in RET-transformed fibroblasts, HEK293 cells, and in primary tumor cells and cell lines from human thyroid cancer,[25] raising the possibility that this inhibitor could impair TNBC growth in our models by targeting other kinases. Since no other group to our knowledge has tested the potential off-target effects in an EphA2-null model, we decided to test the impact of ALW-II-41-27 on EphA2-deficient C3-TAg tumor cells relative to NG-25 analog control. We reasoned that this cell line was a more appropriate model than knockdown human cell lines in which some EphA2 expression persists, and we chose to assess the effects in three-dimensional culture since we could measure

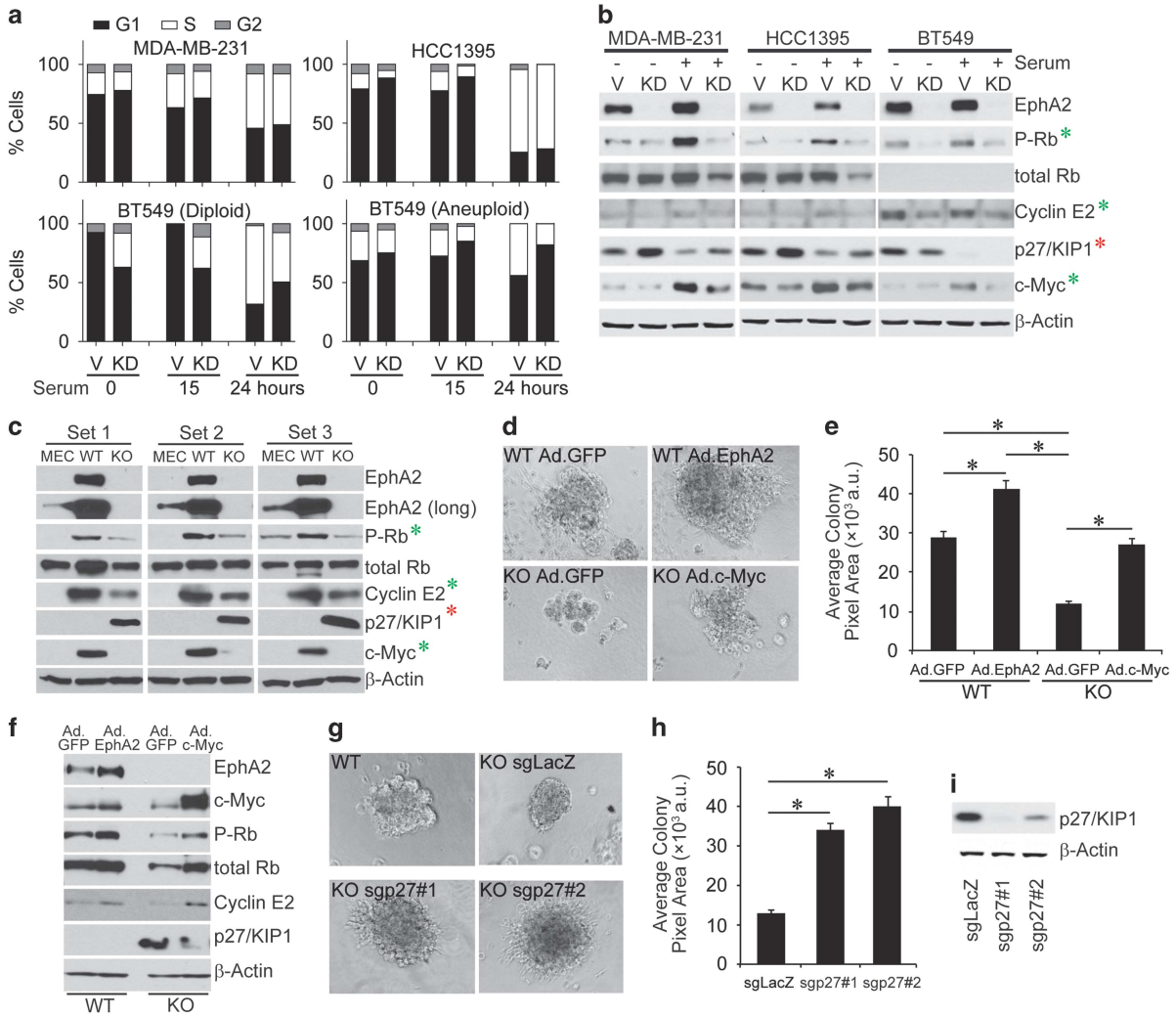

Figure 5. EphA2 loss impairs cell cycle progression through S-phase in TNBC cells. (**a**, **b**) MDA-MB-231, HCC1395 and BT549 vector control (V) and EphA2 shRNA knockdown (KD) lines were starved then serum-stimulated for 0, 15 or 24 h prior to propidium iodide labeling and FACS analysis for DNA content. (**a**) All three human shEphA2 knockdown lines showed a general decrease in the percentage of cells in S-phase relative to vector controls: MDA-MB-231 at 15 h post serum stimulation, HCC1395 at 0 and 15 h post serum stimulation, and aneuploidy BT549 at 0, 15 and 24 h post serum stimulation. (**b**) Immunoblot analysis of S-phase cell cycle regulators in vector (V) control versus EphA2 shRNA knockdown (KD) human TNBC lines under basal (serum-starved, −) conditions versus stimulation with serum (+) for 15 h; (**c**) and three independent isolates of wild-type (WT) and EphA2-deficient (KO) C3-TAg cells versus primary mouse mammary epithelial cells (MEC). We observed decreased levels of P-Rb, c-Myc and cyclin E2 (green *) and increased expression of p27/KIP1 cell cycle inhibitor (red *) in KD and KO cells relative to controls. Data were from three independent experiments. (**d**, **e**) Adenovirus-mediated overexpression of EphA2 (Ad.EphA2) significantly increased colony size of wild-type (WT) C3-TAg cells in three-dimensional spheroid culture relative to adenovirus GFP (Ad.GFP) control (*$P < 0.05$, Student's *t*-test). Overexpression of adenovirus c-Myc (Ad.c-Myc) in EphA2-deficient (KO) C3-TAg cells rescued three-dimensional spheroid growth to near wild-type levels relative to Ad.GFP controls (*$P < 0.05$, Student's *t*-test). (**f**) Immunoblot analyses confirmed EphA2 or c-Myc overexpression as well as modulation of P-Rb, cyclin E2 and p27/KIP1 in WT and KO C3-TAg cells. (**g**, **h**) Stable knockout of p27/KIP1 by two independent guide RNA sequences also rescued growth of KO C3-TAg cells in spheroid culture. (**i**) Immunoblot analysis confirmed p27/KIP1 knockout. *N* = three independent experiments/condition with triplicate biological replicates, (*$P < 0.05$, Student's *t*-test).

colony size (growth) and morphology (malignant/invasive behavior) at the same time. If ALW-II-41-27 targeted other Eph family RTKs or displayed significant off-target effects by inhibiting other kinases, we hypothesized that we would observe a reduction in growth/change in colony morphology in EphA2-deficient lines treated with ALW-II-41-27. ALW-II-41-27 treatment significantly reduced colony size in wild-type C3-TAg three-dimensional spheroid culture (Figures 6f and g), mimicking the effects of EphA2-deficiency. Importantly, the impact of ALW-II-41-27 relative to NG-25 control on EphA2-deficient C3-TAg lines was not significant, suggesting minimal off-target effects for this inhibitor (Figures 6f and g).

To determine the impact of EphA2 targeting in clinically relevant models of TNBC, we treated two independent human TNBC PDX lines[26] that overexpressed EphA2 relative to normal/hyperplastic breast tissue (Figure 6h) with ALW-II-41-27 *in vivo*. PDX tissue was resected from donor animals and serially transplanted into the cleared fat pads of recipient nonobese diabetic-severe combined immunodeficient (NOD-SCID) female mice. When the tumors reached at least 200 mm^3, tumor-bearing animals were randomized into treatment groups, and treated daily with ALW-II-41-27 or vehicle control for 1 week prior to harvest. While vehicle control tumors continued to grow, we observed that ALW-II-41-27 tumor volume remained stable within 3–5 days after

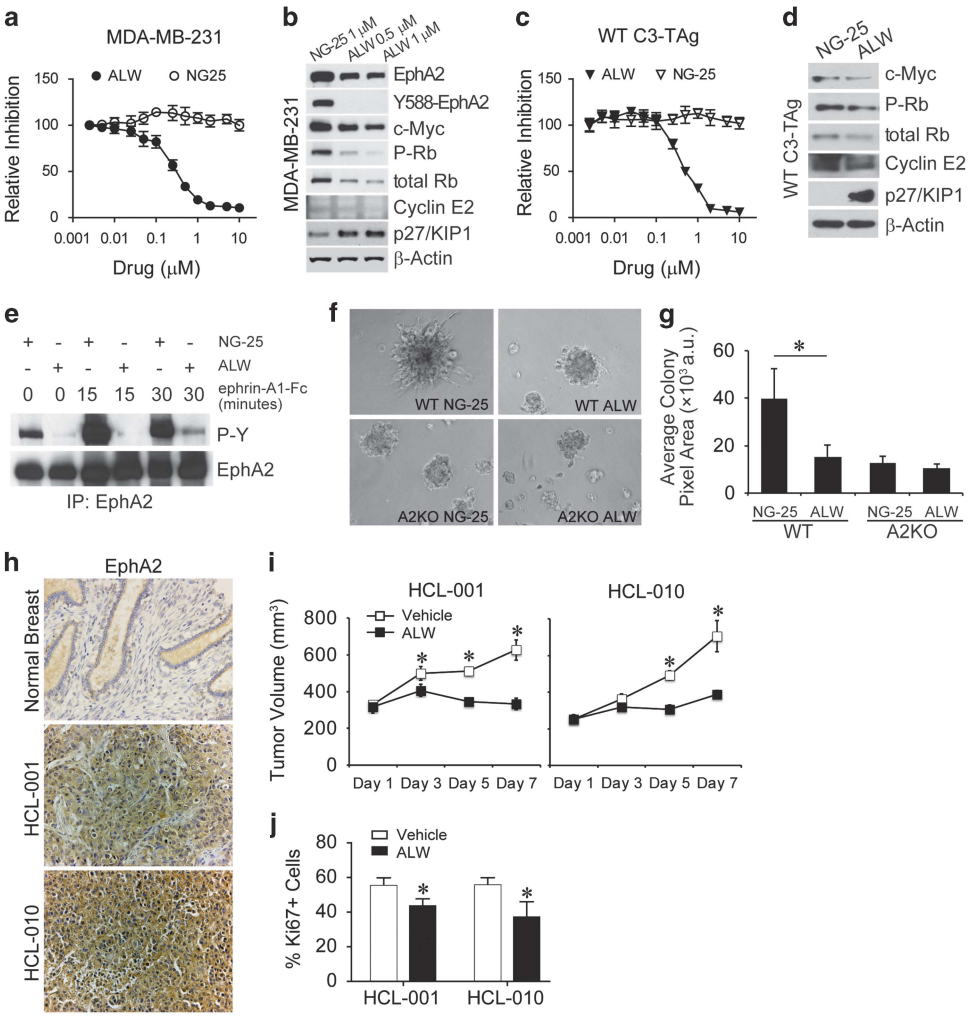

Figure 6. Pharmacologic inhibition of EphA2 recapitulates effects of genetic ablation. (**a**–**c**) MDA-MB-231 and wild-type (WT) C3-TAg tumor cells were grown in the presence of increasing concentrations of an EphA2 small molecule tyrosine kinase inhibitor ALW-II-41-27 (ALW) versus analog control and growth assessed by MTT assay after 72 h in culture. (**a**, **c**) ALW significantly reduced growth in a dose-dependent manner (*$P < 0.05$, Student's *t*-test). (**b**, **d**) ALW treatment reduced basal levels of P-EphA2/EphA2 (**b**, MDA-MB-231 cell line), c-Myc, P-Rb, cyclin E2 and enhanced expression of p27/KIP1 relative to NG-25 control. (**e**) C3-TAg cells were starved and stimulated for 0, 15 and 30 min with ephrin-A1-Fc (EphA2 ligand; 1 μg/ml) in the presence or absence of ALW-II-41-27 or NG-25 control. EphA2 was immunoprecipitated and products probed for tyrosine phosphorylation and EphA2. ALW-II-41-27 significantly reduced basal and ephrin-A1-Fc induced tyrosine phosphorylation. (**f**, **g**) Wild-type (WT) and EphA2-deficient (KO) C3-TAg cells were grown in three-dimensional spheroid culture in the presence of 1 μM EphA2 small molecule inhibitor (ALW-II-41-27) versus analog control (NG-25) for 7 days. (**g**) ALW-II-41-27 significantly reduced colony size in WT cells relative to NG-25, but did not affect growth of KO cells, suggesting minimal off-target effects of the compound. $N =$ three independent experiments/condition with triplicate biological replicates, Student's *t*-test (NG-25 versus ALW WT cells, $P < 0.05$; NG-25 versus ALW KO cells, not significant; Student's *t*-test). (**h**–**j**) Two independent TNBC patient-derived xenograft (PDX) lines were implanted into the cleared fat pads of female NOD-SCID mice. (**h**) These PDX lines overexpressed EphA2 protein relative to normal/hyperplastic/benign human breast tissue controls. (**i**) Once tumors reached a volume $\geqslant 200\ mm^3$, mice were randomized and treated with either vehicle control or ALW-II-41-27 for 7 days. ALW treatment significantly reduced tumor volume over time in both lines (*$P < 0.05$, one-way ANOVA) within 3–5 days after treatment. (**j**) Histologic analyses of tumor sections for proliferation marker revealed a significant decrease in proliferation index (%Ki67$^+$ nuclei/total nuclei; *$P < 0.05$, Student's *t*-test) for ALW-treated tumors relative to controls.

treatment was initiated and persisted through day 7 (Figure 6i; Supplementary Figure S7a), for both HCI-001 and HCI-010 TNBC PDX lines. Tumors from animals treated with ALW-II-41-27 were less cellular than those from control-treated animals (Supplementary Figures S7a and b). Consistent with knockdown studies and treatment of TNBC cell lines *in vitro*, ALW-II-41-27-treated tumors displayed a significant decrease in proliferation (Figure 6j; Supplementary Figure S7c) with no change in apoptosis (Supplementary Figures S7d and e). We also observed decreased protein expression of c-Myc and increased expression of p27/KIP1 in tumor sections from ALW-II-41-27-treated animals versus controls (Supplementary Figure S7f). PDX tumor lysates (HCC-010) showed a significant decrease in EphA2 phosphorylation in animals that received two doses of ALW-II-41-27 versus control-treated animals (Supplementary Figure S7g), validating EphA2 targeting *in vivo*. Thus, therapeutic targeting of EphA2 impairs proliferation coincident with modulation of c-Myc and p27/KIP1 stability in clinically relevant models of human TNBC *in vivo*.

DISCUSSION

While recent studies have linked EphA2 expression and activity to human breast cancer patient outcome,[12] the relative clinical relevance of this RTK in specific breast cancer molecular subtypes

remained under-investigated. Our analysis of human breast cancer data revealed that EphA2 is highly enriched in the basal-like molecular subtype relative to other breast cancer subtypes. Molecular, genetic and pharmacologic targeting of EphA2 significantly reduced tumor cell proliferation in human cell lines, mouse models and PDXs. Loss or inhibition of EphA2 results in elevated levels of the cdk inhibitor p27/KIP1, as well as reduced expression of c-Myc and cyclin E2. EphA2 gain-of-function showed the reverse effect, and both c-Myc overexpression and p27/KIP1 knockout rescued proliferation defects induced by loss of EphA2. As EphA2 loss reduced the percentage of tumor cells in S-phase, our data suggest that EphA2 normally promotes growth in basal-like/TNBCs through p27/KIP1 inhibition-dependent and c-Myc-dependent mechanisms, which in turn activate downstream of cyclin/cdk pathways that advance S-phase. As rapid proliferation is a hallmark of this molecular breast cancer subtype, EphA2 regulation of molecular signaling pathways that control proliferation characterizes this receptor as a clinically relevant target for basal-like/TNBCs, which currently lacks approved molecularly targeted therapies.

While no published reports, to our knowledge, validate amplification of the gene encoding *EPHA2* or *ephA2* messenger RNA in the HCI-001 or HCI-010 lines used in our study, a recent report from Zena Werb's laboratory showed lower expression of *c-myc* and *cdk2* in poorly metastatic cells isolated from HCI-001 and HCI-010.[27] These data validate expression of relevant pathway components in these models that our data link to EphA2. In addition, both lines exhibited loss of *PTEN* expression. As activation of the PI3K pathway in breast cancer, including the basal/triple-negative subtype, elevates EphA2 expression,[28] this could represent a genetic vulnerability that might enable response to anti-EphA2 therapy. We are actively exploring the potential link between PI3K activation and EphA2 elevation in TNBC.

Other recent studies support the clinical relevance of EphA2 in basal-like breast cancer. Analysis of basal-like human breast cancer cell lines revealed elevated levels of phosphorylated EphA2, as well as elevated Met, Src family kinases and FAK phosphorylation, in BT549 and MDA-MB-231,[29] consistent with our data. Overall survival in a cohort of basal-like breast cancer patients was reported to be significantly lower in patients expressing high *ephA2* messenger RNA levels.[30] In addition, profiling studies in a large panel of human breast cancer cell lines revealed high levels of EphA2 protein in BT549 and MDA-MB-231 concomitant with low levels of ephrin-A1 protein expression,[9] consistent with our analysis of messenger RNA expression analysis in The Cancer Genome Atlas human breast cancer patient data sets. Coupled with our functional studies in human cell lines, the C3-TAg transgenic model of basal-like breast cancer and TNBC PDX models, these data provide a strong rationale for investigating the therapeutic value of EphA2 targeting in this molecular breast cancer subtype.

EphA2 modulates signaling pathways relevant to TNBC proliferation. One such downstream target is the transcription factor c-Myc, which heterodimerizes with its binding partner Max and mediates transcription of genes that regulate growth, invasion and metabolism.[31] Amplification of c-myc has been detected in human TNBC.[32–34] Transcriptional activity of c-Myc promotes expression of genes that drive proliferation, including G_1/S cyclin-dependent kinases and cyclins.[31,35] While p27/KIP1 and cyclin E2 are not direct transcriptional targets, c-Myc regulates transcription of cyclin D2 and cdk4, which can sequester p27/KIP1 to enable activation of cdk2/cyclin E complexes, as well as CUL1 and CKS, which promote proteasome-mediated degradation of p27/KIP1.[35] Both cdk2/cylcin E1 and cdk2/cyclin E2 kinase activities are increased in breast cancer compared to normal tissue, and both cyclin E1 and cyclin E2 negatively correlate with and metastasis-free survival, which is particularly strong for cyclin E2.[36] Thus, reduced c-Myc expression upon EphA2 targeting in TNBC may alleviate repression of p27/KIP1 and subsequently block activity of cyclin E2 associated cdks. Indeed, c-Myc overexpression in EphA2-deficient C3-TAg cell lines significantly reduced p27/KIP1 levels, while increasing expression of cyclin E2 (Figure 5f).

Stability and activation of c-Myc can be regulated by phosphorylation at Ser62 by the Ras/Erk signaling pathway, or at Thr58 by the PI3K/Akt pathway, which enables c-Myc to accumulate in proliferating cells.[37,38] EphA2 is known to activate both Ras/Erk and PI3K/Akt in breast cancer models,[9,10] and consistent with these data, we observed reduced levels of P-Erk and P-Akt in EphA2 knockdown or deficient cell lines relative to controls. Interestingly, we did not observe any reduction in c-Myc phosphorylation in EphA2-deficient cells or cells treated with the EphA2 inhibitor (data not shown). It will be of great interest to identify alternate molecular signaling pathways that link EphA2 to c-Myc expression and/or stability in basal-like/TNBC proliferation, which is a major focus of our ongoing investigation. c-Myc is also associated with metabolic reprogramming in breast cancer, including TNBC.[39,40] Given that EphA/ephrin-A1 signaling was recently linked to glutamine metabolism in HER2-positive breast cancer models,[41] it will be also of great interest to explore the potential link between EphA2 and c-Myc-regulated metabolism in TNBC.

In addition to c-Myc-mediated p27/KIP1 suppression and cyclin E2 stabilization, c-Myc also cross-talks with the retinoblastoma (Rb) tumor suppressor pathway to regulate TNBC proliferation. Rb canonical function involves inhibition of E2F family transcription factors. Mitogenic signals lead to hyperphosphorylation of Rb and subsequent degradation, which liberates E2F transcription factors to induce expression of cell cycle progression genes.[21] As c-Myc also mediates transcription of cell cycle progression genes, these pathways can cooperate to promote proliferation. In TNBC models, c-Myc overexpression combined with loss of Rb and p53 drove rapid cell growth, and human TNBC tumors that express high levels of Myc and are devoid of Rb have a particularly poor outcome.[42] EphA2 loss of function reduced phosophorylated Rb levels in the C3-TAg model, which is driven by SV40 large T-antigen disruption of Rb-E2F interactions,[43] as well as in human TNBC models with other primary oncogenic drivers (for example, mutant p53 and PTEN deletion in BT549; mutant p53 and mutant K-Ras in MDA-MB-231; mutant p53 in HCC1395).[44] Thus, regulation of Rb function represents another clinically relevant pathway by which EphA2 regulates cell proliferation in TNBC.

In summary, we provide the first evidence that molecular, genetic and pharmacologic EphA2 inhibition reduces proliferation in clinically relevant mouse and human models of basal-like/TNBC through modulation of cell cycle regulators including c-Myc and p27/KIP1. Targeting EphA2 represents a new therapeutic strategy for treating patients with basal-like/TNBC.

MATERIALS AND METHODS

Reagents

Antibodies against the following proteins were used: EphA2 (Zymed Laboratories, Burlingame, CA, USA; Santa Cruz Biotechnology, Santa Cruz, CA, USA; EMD Millipore, Billerica, MA, USA); β-actin, phosphotyrosine (PY99 and PY20, Santa Cruz Biotechnology); P-EphA2 Tyr588, c-Myc, p27/KIP1, cyclin E2, cyclin B1, p53, phospho/total Rb, phospho/total cdk2, phopsho/total Erk, phospho/total Akt (Cell Signaling Technology, Danvers, MA, USA); mouse monoclonal anti-c-Myc (clone 9E10, Sigma-Aldrich, St Louis, MO, USA); BrdU (Sigma-Aldrich). Growth factor-reduced Matrigel was purchased from BD Biosciences (San Jose, CA, USA). Ephrin-A1-Fc was purchased from R&D Systems (Minneapolis, MN, USA). Adenovirus harboring EphA2 was described previously.[45] Adenoviruses harboring c-Myc and GFP were purchased from Vector Biolabs (Malvern, PA, USA). 4′,6-diamidino-2 phenylindole dihydrochloride (DAPI) nuclear stains were purchased from Invitrogen (Carlsbad, CA, USA), and Sigma-Aldrich, respectively. 5-bromo-2-deoxyuridine (BrdU) was purchased from Sigma-Aldrich. Apoptag Red

In Situ Apotosis Detection and MTT Growth Assay kits were purchased from EMD Millipore. M.O.M. (mouse-on-mouse) kit was purchased from Vector Laboratories (Burlingame, CA, USA). Human TNBC TMAs (BR487b) were purchased from US Biomax, Inc. (Rockville, MD, USA). ALW-II-41-27 and NG-25 were purchased from MedChem Express (Monmouth Junction, NJ, USA). PDX models[26] were obtained from the Huntsman Cancer Institute (Salt Lake City, UT, USA).

Expression analyses in data from patients and TMAs

RNAseq_v2 data (level 3) from the The Cancer Genome Atlas breast cancer cohort ($n = 1177$) were downloaded from the The Cancer Genome Atlas data portal and analyzed for intrinsic molecular subtype using the genefu package in R.[46] Log2 normalized gene expression data for *EPHA2* and *EFNA1* were extracted and used to construct a ratio (*EPHA2-EFNA1*) for comparison across molecular subtypes. Kaplan–Meier analysis of data set with microarray profiles from 316 ER^-/PR^- human basal-like breast cancer samples was performed using KMplot.com,[14] selecting for the upper tertile with highest *EphA2* levels. Expression levels were analyzed in relation to RFS probability using log-rank and Cox analyses. For commercial TNBC TMAs, relative EphA2, c-Myc and p27/KIP1 expression in 48 independent samples was scored using a continuous scale as follows: 0 = 0–10% positive tumor epithelium, 1 = 10–25% positive tumor epithelium, 2 = 25–50% positive tumor epithelium and 3 ⩾ 50% positive tumor epithelium/core. For EphA2 expression analyses, EphA2 protein expression in TNBC cores were compared to expression in normal/hyperplastic and benign fibroadenoma control samples from Cybrdi TMA CC08-10-001.[12] TMA cores were scored blind by three independent individuals, the average of which was reported here. Differential expression between tissue samples was quantified and statistically analyzed using Fisher's exact test.

Animal studies

All animals were housed under pathogen-free conditions, and experiments were performed in accordance with AAALAC guidelines and with Vanderbilt University Institutional Animal Care and Use Committee approval. C3-TAg mice (FVB) were purchased from Jackson Laboratories (Bar Harbor, ME, USA) and have been described previously.[15,16] C3-TAg-positive males were crossed with EphA2-deficient female FVB congenic mice[10] to generate EphA2 wild-type, heterozygous and deficient C3-TAg-positive female littermate cohorts for analyses. Tumors were collected and volume calculated from caliper measurements as described previously.[10] For xenograft and PDX studies, 3–4-week-old athymic nude female mice and 3–4-week-old NOD-SCID female mice were purchased from Envigo (Indianapolis, IN, USA) and housed under sterile, pathogen-free conditions.

Histologic analyses

Hemotoxylin and eosin staining and immunohistochemistry for Ki67 (proliferation), cleaved caspase 3 (apoptosis) and CD31 (microvascular density) was performed by the Vanderbilt University Translational Pathology Shared Resource. Immunohistochemistry for p27/KIP1 and c-Myc was performed as described previously[10] using rabbit anti-p27/KIP1 antibody (clone D69C12, Cell Signaling Technology, 1:200 overnight at 4 °C) and mouse anti-c-Myc (clone 9E10, Sigma-Aldrich, 1:100 overnight at 4 °C following mouse-on-mouse blocking reagent pre-treatment). Photomicrographs were captured using an Olympus BX60 stereomicroscope with Olympus DP72 digital camera (Olympus, Center Valley, PA, USA). Quantification of proliferation/apoptosis indices and microvascular density were performed on ×20 photomicrographs using CellSens software. Immunohistochemistry staining for EphA2 was performed as described previously[10] using Zymed anti-EphA2 antibody (Thermo Fisher Scientific, Waltham, MA, USA Catalog#: 34-7400), 10 μg/ml, overnight, 4 °C.

Cell culture

MDA-MB-231, BT549, HCC1395, HCC1937, HCC1806 and HBL-100 were purchased from the American Type Culture Collection (ATCC, Manassas, VA, USA) and cultured according to the suppliers recommended conditions. The three lines (MDA-MB-231, HCC1395, BT549) selected for proliferation/apoptosis, three-dimensional spheroid culture, FACS and MTT assays were cultured in DMEM supplemented with penicillin–streptomycin and 10% fetal bovine serum. Primary C3-TAg lines derived from wild-type and EphA2-deficient C3-TAg mice were collected as described previously.[10] Immortalized cells were generated by serial passage of primary cells and selection of surviving colonies. C3-TAg cells were maintained in DMEM/10% fetal bovine serum. For some experiments, cells were starved in Opti-MEM media supplemented with 0.1% fetal bovine serum prior to experimental manipulation. EphA2 stable shRNA knockdown lines were generated by infecting TNBC cells with lentiviruses harboring pLKO.1 puro vector (Addgene, Cambridge, MA, USA) or vector harboring human EphA2 shRNA targeting sequences (#1 CGGACAGACATATGGGATATT) #2 GCGTA TCTTCATTGAGCTCAA)/control GFP targeting sequences (GCAAGCTGA CCCTGAAGTTCAT) and selecting with puromycin (2 μg/ml). Knockdown was confirmed by immunoblot analysis.

Growth and apoptosis assays

BrdU incorporation and TUNEL analyses in cultured control versus EphA2 knockdown TNBC cell lines were performed as described previously.[10,20] Photomicrographs were captured using an Olympus BX60 stereomicroscope with Olympus DP72 digital camera and CellSens software. CellSens software was used for quantification of the percentage $BrdU^+/TUNEL^+$ nuclei relative to total nuclei in viewing fields. For MTT Assays, 3×10^3 control and EphA2 knockdown cells were plated into 96-well plates with at least four replicates in growth media. On day 1, 2, 4, 6 and 8, MTT reagent was added and plates were read using Synergy HT Multi-Mode Reader (BioTek, Winooski, VT, USA). Cell growth or survival was normalized to day 1 or control cells. To evaluate cell growth inhibition with EphA2 inhibitor, different doses of ALW-II-41-27 or analog control NG-25 (2.5 nM–10 μM) were added into wells after attachment of cells (4×10^3) to the bottom plates. After 3 days incubation, the MTT assay was performed. Three-dimensional spheroid cultures of control and EphA2 knockdown TNBC lines on Matrigel were established and grown as described previously. For three-dimensional spheroid culture studies in the C3-TAg model, primary C3-TAg tumor cells and lines established from wild-type and EphA2-deficient C3-TAg tumors were plated at low density on growth factor-reduced Matrigel and grown as described previously.[10] For some studies, cultures were treated with ALW-II-41-27 or analog control NG-25 (0.5–1 μM). CRISPR/Cas9 guide RNA-mediated p27/KIP1 knockout lines were generated from EphA2-deficient C3-TAg parental lines via lentiviral transduction as described above (guide RNA#1 TCAAACGTGAGA GTGTCTAA, guide RNA#2, CTTGGGGTGCTCCGCTTGTC) and grown in three-dimensional spheroid culture compared to control LacZ targeting lines (guide RNA TGCGAATACGCCCACGCGAT). Photomicrographs were captured using an Olympus IX71 inverted microscope with Olympus DP72 digital camera. Colony size was measured in ×10 photomicrographs using NIH Image J software (NIH, Bethesda, MD, USA).

Fluorescence activated cell sorting

EphA2 knockdown or control TNBC lines were serum-starved for 24 h and released back to growth media for 0, 15 and 24 h. Cells were trypsinized, washed twice with cold PBS and fixed in 80% ice-cold EtOH. For cell cycle analysis, cell pellets were washed again with cold PBS and incubated in PBS with propidium iodide (50 μg/ml), RNase A (50 μg/ml), Triton X-100 (0.1%) and EDTA disodium (0.1 mM) for 30 min at room temperature. Single cell suspensions were analyzed on BD LSR II Flow Cytometer (BD Biosciences). ModFit LT software (Verity Software House, Topsham, ME, USA) was used to analyze the DNA patterns and cell cycle stages.

Immunoblot and immunoprecipitation

Immunoblot analyses were performed on 25–50 μg of cell line or tumor tissue lysates collected as described previously[10] using chemiluminescence or LI-COR Odyssey detection systems. EphA2 was immunoprecipitated from 500 μg cell lysate (using 0.5 μg anti-EphA2 C-20/SC-924, Santa Cruz Biotechnology, plus 0.5 μg anti-EphA2, D7, EMD Millipore followed by A/G PLUS-Agarose beads, Santa Cruz Biotechnology) collected from C3-TAg cell lines serum-starved and stimulated with 1 μg/ml ephrin-A1-Fc for indicated times in the presence or absence of 1 μM NG-25 or ALW-II-27-41. Antibodies/conditions for immunoblot were as follows: rabbit anti-EphA2 C-20 (Santa Cruz Biotechnology, #SC-924), 1:1,000; goat anti-β-actin I-19 (Santa Cruz Biotechnology, #SC-1616) 1:1,000; rabbit anti-phospho-EphA2 D7X2L (Cell Signaling Technology, P-EphA2 Tyr588, #12677) 1:1000; mouse anti-phosphotyrosine PY99 and PY20 (Santa Cruz Biotechnology, PY99 #SC-7020 and PY20 #SC-508) mixed 1:1000 each; rabbit anti-c-Myc D84C12 (Cell Signaling Technology, #5605) 1:1000; rabbit anti-p27/KIP1* D69C12 (Cell Signaling Technology, #3686) 1:200; rabbit anti-cyclin E2* (Cell Signaling, #4132) 1:500; rabbit anti-cyclin B1 D5C10 (Cell Signaling Technology, #12231) 1:1000; rabbit anti-p53 (Cell Signaling, #2572) 1:500;

phospho/total Rb (Cell Signaling Technology, P-Rb Ser795 #9301; Rb #9313) 1:500; rabbit anti-phospho/total cdk2 (Cell Signaling, P-cdk2 Thr160, #2561; cdk2 782B #2546) 1:1000; rabbit anti-phospho/total Akt (Cell Signaling Technology, P-Akt Ser473 193H12 #4058; Akt #9272) 1:1000; rabbit anti-phospho/total Erk 1/2 (Cell Signaling Technology, P-Erk Thr202/204 D13.14.4E #4307; Erk #9102) 1:1000. Antibodies were diluted in TBST/5% nonfat milk or *TBST/5% bovine serum albumin and incubated overnight at 4 °C. Secondary antibodies were diluted 1:5000 or *1:3000 in TBST/5% milk and incubated 1 h at room temperature. Signal was detected using Clarity (Bio-Rad) or *West Pico (Thermo Fisher Scientific) ECL substrate. For some blots, secondary IRDye 680LT or 800CW secondary antibodies (LI-COR Biotechnology, Atlanta, GA, USA) diluted 1:10000 were used to detect protein signals using a LI-COR Odyssey Infrared Imaging System.

Xenograft/PDX and drug studies *in vivo*

For cell line xenograft studies, 3–4-week-old nude female mice were injected orthotopically into the inguinal mammary fat pad with 2.5×10^6 MDA-MB-231 or BT549 in 100 µl 1:1 growth factor-reduced Matrigel/PBS. The left flank received control shRNA cells and the contralateral flank (right) received EphA2 shRNA knockdown cells. Mice were monitored for tumor growth and tumors were measured by digital caliper to determine volume (volume = length × width^2 × 0.52).[10] Tumors were grown for 2 weeks prior to harvest, and analyses for proliferation (Ki67), apoptosis (Cl. Caspase 3) and microvascular density (CD31) were performed as described above.

For PDX studies, 2 mm^3 portions of cryopreserved tissue were implanted in the surgically cleared inguinal mammary fat pads of 3–4-week-old NOD-SCID recipient female mice. HCI-001 and HCI-010 TNBC-derived lines were used.[10] When the initial tumors reached 1 cm^3, tumors were collected, cut into 2 mm^3 portions and serially transplanted into the surgically cleared inguinal mammary fat pads of 3–4-week-old NOD-SCID recipient female mice to establish cohorts. Tumors were allowed to engraft and grow to at least 200 mm^3, randomized into cohorts (simple randomization by having a blinded laboratory technician randomly divide mice from single cages into separate cages for vehicle control treatment versus ALW treatment without assessing the size of orthotopic mammary tumors), and injected intraperitoneally twice daily for 1 week with vehicle control or 15 mg/kg ALW-II-41-37 in 10% 1-methyl-2-pyrrolidinone and 90% polyethylene glycol 300.[22] Tumors were measured four times weekly and tumor volume calculated as described above. At the end of the treatment period, tumors were collected and analyzed for proliferation, apoptosis and microvascular density as described above. An independent cohort of HCC-010 PDX tumor-bearing animals was treated with two doses (at 0 and 8 h) with vehicle versus ALW-II-41-37. Tumors were collected 1 h following final treatment to validate EphA2 targeting. Tumor lysates were generated and EphA2 immunoprecipitated as described above. Lysates and IP products were probed for phospho-EphA2 (Tyr588) as described above, and blots were stripped and reprobed for total EphA2 as described above.

In order to maintain the overall health of NOD-SCID hosts and to minimize the potential for pain and suffering/risking loss of animals due to death prior to the end of the experiment, we chose to allow tumors to reach a maximum volume of 800–900 mm^3, which enabled us to successfully assess the efficacy of treatment while still maintaining humane end points.

Statistical methods/analyses

For all *in vitro* and *in vivo* analyses, center values represent the mean. Error bars represent s.d. for *in vitro* studies and s.e.m. for *in vivo* studies. Variance observed was similar between groups that were statistically compared for all experiments. Statistical significance for *in vitro* analyses was determined using two-tailed, unpaired Student *t*-tests. Statistical significance for tumor volume analyses in C3-TAg transgenic animals and PDX studies was determined using one-way analysis of variance. As noted in figure legends, cell line/cell culture studies were performed in three independent experiments using three biological replicates/experiment. $N = 5$ independent tumors (shControl versus contralateral shEphA2) for MDA-MB-231 and BT549 xenografts. Sample sizes were selected based on previous studies using other transplantable xenograft/allograft models in which EphA2 expression/function was impaired.[10,17,20,47] $N = 9$ EphA2$^{+/+}$, 11 EphA2$^{+/-}$, and 9 EphA2$^{-/-}$ for C3-TAg transgenic studies. To determine the minimum number of mice required for these studies, power analysis was performed using data from similar preliminary studies with simulation of a mixed effects model, which specified fixed treatment effect and random effect for intercept and time. The model adjusted for variations in baseline tumor volume. Bonferroni adjustment was used for multiple comparisons. The simulation indicated that a minimum of nine mice per group would be needed to detect a treatment slope (tumor volume/time) difference of 16 (mm^3/week) with an 80% power at a two-sided type I error of 5%. Therefore, the effect size will see a 96 mm^2 difference in mean tumor volume between two groups. $N = 5$ independent tumors/treatment group for each TNBC PDX tumor treated with vehicle control versus ALW-II-41-27. As noted for MDA-MB-231 and BT549 xenografts, sample sizes were selected based on previous studies using other transplantable xenograft/allograft models in which EphA2 expression/function was impaired.[10,17,20,47] For tumor volume analyses (xenograft and transgenic models), laboratory staff member measuring volume was blinded to the genotype/treatment group designation for each animal.

CONFLICT OF INTEREST

The authors declare no conflict of interest.

ACKNOWLEDGEMENTS

We thank Dr Bojana Jovanovic (Dana-Farber Cancer Institute) and Dr Tammy Sobolik (Vanderbilt University) for helpful discussions on the research. This work was supported by NIH/NCI Grants R01 CA148934 (DMB-S); R01 CA177681, and R01 CA95004 (JC). Acquisition of PDX models from the Huntsman Cancer Institute was supported by CTSA award UL1TR000445 (via Vanderbilt Institute of Clinical and Translational Research (VICTR) Grant VR10608 (DMB-S)) from the National Center for Advancing Translational Sciences. Its contents are solely the responsibility of the authors and do not necessarily represent official views of the National Center for Advancing Translational Sciences or the National Institutes of Health. JC is also supported by US Department of Veterans Affairs VA Merit Award (5I01BX000134). This work was also supported in part by the NCI Cancer Center Support Grant # P30 CA068485 utilizing the Translational Pathology Shared Resources.

REFERENCES

1 Foulkes WD, Reis-Filho JS, Narod SA. Tumor size and survival in breast cancer–a reappraisal. *Nat Rev Clin Oncol* 2010; **7**: 348–353.
2 Zardavas D, Irrthum A, Swanton C, Piccart M. Clinical management of breast cancer heterogeneity. *Nat Rev Clin Oncol* 2015; **12**: 381–394.
3 Fosu-Mensah N, Peris MS, Weeks HP, Cai J, Westwell AD. Advances in small-molecule drug discovery for triple-negative breast cancer. *Future Med Chem* 2015; **7**: 2019–2039.
4 Lehmann BD, Pietenpol JA. Clinical implications of molecular heterogeneity in triple negative breast cancer. *Breast* 2015; **24**(Suppl 2): S36–S40.
5 Le Du F, Eckhardt BL, Lim B, Litton JK, Moulder S, Meric-Bernstam F *et al.* Is the future of personalized therapy in triple-negative breast cancer based on molecular subtype? *Oncotarget* 2015; **6**: 12890–12908.
6 Kullander K, Klein R. Mechanisms and functions of Eph and ephrin signaling. *Nat Rev Mol Cell Biol* 2002; **3**: 475.
7 Pasquale EB. Developmental cell biology: Eph receptor signalling casts a wide net on cell behaviour. *Nat Rev Mol Cell Biol* 2005; **6**: 462–475.
8 Pasquale EB. Eph-ephrin bidirectional signaling in physiology and disease. *Cell* 2008; **133**: 38–52.
9 Macrae M, Neve RM, Rodriguez-Viciana P, Haqq C, Yeh J, Chen C *et al.* A conditional feedback loop regulates Ras activity through EphA2. *Cancer Cell* 2005; **8**: 111–118.
10 Brantley-Sieders DM, Zhuang G, Hicks D, Fang WB, Hwang Y, Cates JM *et al.* The receptor tyrosine kinase EphA2 promotes mammary adenocarcinoma tumorigenesis and metastatic progression in mice by amplifying ErbB2 signaling. *J Clin Invest* 2008; **118**: 64–78.
11 Larsen AB, Pedersen MW, Stockhausen MT, Grandal MV, van Deurs B, Poulsen HS. Activation of the EGFR gene target EphA2 inhibits epidermal growth factor-induced cancer cell motility. *Mol Cancer Res* 2007; **5**: 283–293.
12 Brantley-Sieders DM, Jiang A, Sarma K, Badu-Nkansah A, Walter DL, Shyr Y *et al.* Eph/ephrin profiling in human breast cancer reveals significant associations between expression level and clinical outcome. *PLoS One* 2011; **6**: e24426.
13 Parker JS, Mullins M, Cheang MC, Leung S, Voduc D, Vickery T *et al.* Supervised risk predictor of breast cancer based on intrinsic subtypes. *J Clin Oncol* 2009; **27**: 1160–1167.
14 Gyorffy B, Lanczky A, Eklund AC, Denkert C, Budczies J, Li Q *et al.* An online survival analysis tool to rapidly assess the effect of 22,277 genes on breast cancer

prognosis using microarray data of 1,809 patients. *Breast Cancer Res Treat* 2010; **123**: 725–731.
15 Green JE, Shibata MA, Yoshidome K, Liu ML, Jorcyk C, Anver MR *et al.* The C3(1)/SV40 T-antigen transgenic mouse model of mammary cancer: ductal epithelial cell targeting with multistage progression to carcinoma. *Oncogene* 2000; **19**: 1020–1027.
16 Maroulakou IG, Anver M, Garrett L, Green JE. Prostate and mammary adenocarcinoma in transgenic mice carrying a rat C3(1) simian virus 40 large tumor antigen fusion gene. *Proc Natl Acad Sci USA* 1994; **91**: 11236–11240.
17 Brantley-Sieders DM, Fang WB, Hicks DJ, Zhuang G, Shyr Y, Chen J. Impaired tumor microenvironment in EphA2-deficient mice inhibits tumor angiogenesis and metastatic progression. *FASEB J* 2005; **19**: 1884–1886.
18 Guo Z, He B, Yuan L, Dai W, Zhang H, Wang X *et al.* Dual targeting for metastatic breast cancer and tumor neovasculature by EphA2-mediated nanocarriers. *Int J Pharm* 2015; **493**: 380–389.
19 Vaught D, Chen J, Brantley-Sieders DM. Regulation of mammary gland branching morphogenesis by EphA2 receptor tyrosine kinase. *Mol Biol Cell* 2009; **20**: 2572–2581.
20 Brantley-Sieders DM, Dunaway CM, Rao M, Short S, Hwang Y, Gao Y *et al.* Angiocrine factors modulate tumor proliferation and motility through EphA2 repression of Slit2 tumor suppressor function in endothelium. *Cancer Res* 2011; **71**: 976–987.
21 Hutcheson J, Witkiewicz AK, Knudsen ES. The RB tumor suppressor at the intersection of proliferation and immunity: relevance to disease immune evasion and immunotherapy. *Cell Cycle* 2015; **14**: 3812–3819.
22 Amato KR, Wang S, Hastings AK, Youngblood VM, Santapuram PR, Chen H *et al.* Genetic and pharmacologic inhibition of EPHA2 promotes apoptosis in NSCLC. *J Clin Invest* 2014; **124**: 2037–2049.
23 Amato KR, Wang S, Tan L, Hastings AK, Song W, Lovly CM *et al.* EPHA2 blockade overcomes acquired resistance to EGFR kinase inhibitors in lung cancer. *Cancer Res* 2016; **76**: 305–318.
24 Choi Y, Syeda F, Walker JR, Finerty Jr PJ, Cuerrier D, Wojciechowski A *et al.* Discovery and structural analysis of Eph receptor tyrosine kinase inhibitors. *Bioorg Med Chem Lett* 2009; **19**: 4467–4470.
25 Moccia M, Liu Q, Guida T, Federico G, Brescia A, Zhao Z *et al.* Identification of novel small molecule inhibitors of oncogenic RET kinase. *PLoS One* 2015; **10**: e0128364.
26 DeRose YS, Wang G, Lin YC, Bernard PS, Buys SS, Ebbert MT *et al.* Tumor grafts derived from women with breast cancer authentically reflect tumor pathology, growth, metastasis and disease outcomes. *Nat Med* 2011; **17**: 1514–1520.
27 Lawson DA, Bhakta NR, Kessenbrock K, Prummel KD, Yu Y, Takai K *et al.* Single-cell analysis reveals a stem-cell program in human metastatic breast cancer cells. *Nature* 2015; **526**: 131–135.
28 Young CD, Zimmerman LJ, Hoshino D, Formisano L, Hanker AB, Gatza ML *et al.* Activating PIK3CA mutations induce an EGFR/ERK paracrine signaling axis in basal-like breast cancer. *Mol Cell Proteomics* 2015; **14**: 1959–1976.
29 Hochgrafe F, Zhang L, O'Toole SA, Browne BC, Pinese M, Porta Cubas A *et al.* Tyrosine phosphorylation profiling reveals the signaling network characteristics of basal breast cancer cells. *Cancer Res* 2010; **70**: 9391–9401.
30 Tsouko E, Wang J, Frigo DE, Aydogdu E, Williams C. miR-200a inhibits migration of triple-negative breast cancer cells through direct repression of the EPHA2 oncogene. *Carcinogenesis* 2015; **36**: 1051–1060.
31 Hartl M. The quest for targets executing MYC-dependent cell transformation. *Front Oncol* 2016; **6**: 132.
32 Dillon JL, Mockus SM, Ananda G, Spotlow V, Wells WA, Tsongalis GJ *et al.* Somatic gene mutation analysis of triple negative breast cancers. *Breast* 2016; **29**: 202–207.
33 Murria R, Palanca S, de Juan I, Alenda C, Egoavil C, Segui FJ *et al.* Immunohistochemical, genetic and epigenetic profiles of hereditary and triple negative breast cancers. Relevance in personalized medicine. *Am J Cancer Res* 2015; **5**: 2330–2343.
34 Weisman PS, Ng CK, Brogi E, Eisenberg RE, Won HH, Piscuoglio S *et al.* Genetic alterations of triple negative breast cancer by targeted next-generation sequencing and correlation with tumor morphology. *Mod Pathol* 2016; **29**: 476–488.
35 Pelengaris S, Khan M, Evan G. c-MYC: more than just a matter of life and death. *Nat Rev Cancer* 2002; **2**: 764–776.
36 Caldon CE, Musgrove EA. Distinct and redundant functions of cyclin E1 and cyclin E2 in development and cancer. *Cell Div* 2010; **5**: 2.
37 Meyer N, Penn LZ. Reflecting on 25 years with MYC. *Nat Rev Cancer* 2008; **8**: 976–990.
38 Sears R, Nuckolls F, Haura E, Taya Y, Tamai K, Nevins JR. Multiple Ras-dependent phosphorylation pathways regulate Myc protein stability. *Genes Dev* 2000; **14**: 2501–2514.
39 Shen L, O'Shea JM, Kaadige MR, Cunha S, Wilde BR, Cohen AL *et al.* Metabolic reprogramming in triple-negative breast cancer through Myc suppression of TXNIP. *Proc Natl Acad Sci USA* 2015; **112**: 5425–5430.
40 Terunuma A, Putluri N, Mishra P, Mathe EA, Dorsey TH, Yi M *et al.* MYC-driven accumulation of 2-hydroxyglutarate is associated with breast cancer prognosis. *J Clin Invest* 2014; **124**: 398–412.
41 Youngblood VM, Kim LC, Edwards DN, Hwang Y, Santapuram PR, Stirdivant SM *et al.* The ephrin-A1/EPHA2 signaling axis regulates glutamine metabolism in HER2-positive breast cancer. *Cancer Res* 2016; **76**: 1825–1836.
42 Knudsen ES, McClendon AK, Franco J, Ertel A, Fortina P, Witkiewicz AK. RB loss contributes to aggressive tumor phenotypes in MYC-driven triple negative breast cancer. *Cell Cycle* 2015; **14**: 109–122.
43 Sullivan CS, Cantalupo P, Pipas JM. The molecular chaperone activity of simian virus 40 large T antigen is required to disrupt Rb-E2F family complexes by an ATP-dependent mechanism. *Mol Cell Biol* 2000; **20**: 6233–6243.
44 Chavez KJ, Garimella SV, Lipkowitz S. Triple negative breast cancer cell lines: one tool in the search for better treatment of triple negative breast cancer. *Breast Dis* 2010; **32**: 35–48.
45 Brantley-Sieders DM, Caughron J, Hicks D, Pozzi A, Ruiz JC, Chen J. EphA2 receptor tyrosine kinase regulates endothelial cell migration and vascular assembly through phosphoinositide 3-kinase-mediated Rac1 GTPase activation. *J Cell Sci* 2004; **117**: 2037–2049.
46 Haibe-Kains B. genefu R package: relevant functions for gene expression analysis, especially in breast cancer. Available at: http://www.bioconductor.org/packages/release/bioc/html/genefu.html (accessed on 5 October 2016).
47 Brantley DM, Cheng N, Thompson EJ, Lin Q, Brekken RA, Thorpe PE *et al.* Soluble Eph A receptors inhibit tumor angiogenesis and progression in vivo. *Oncogene* 2002; **21**: 7011–7026.

Supplementary Information accompanies this paper on the Oncogene website (http://www.nature.com/onc)